Shahid Bahonar University of Kerman
Journal of Mahani Mathematical Research Center
Print ISSN: 2251-7952 Online ISSN: 2645-4505

THE ROTHE-NEWTON APPROACH TO SIMULATE THE VARIABLE COEFFICIENT CONVECTION-DIFFUSION EQUATIONS

H.M. Srivastava* and M. Izadi

Article type: Research Article
(Invited paper, Received: 14 May 2022, Accepted: 22 May 2022)
(Available Online: 22 May 2022)
(Communicated by A. Borumand Saeid)

Abstract. The current article presents a novel hybrid approach based on the Rothe time-marching algorithm and a spectral matrix collocation approach using the well-known Newton bases to deal with the spatial variable. Utilizing the Rothe approach converts the underlying convection-diffusion into initial-boundary value problems and then the Newton collocation method solves the continuous discretized time equation in each time step. The error analysis of the newly employed basis functions is established. Three numerical simulations are developed to show the accuracy and utility of the proposed hybrid strategy. Applying the current study to other linear and nonlinear PDEs and high-order PDEs can be performed straightforwardly.

Keywords: Convection-diffusion equation, Collocation method, Convergence analysis, Newton bases, Rothe method.
2020 MSC: 65M70, 65M12, 65M20, 65N40.

1. Introduction

Modeling various real-world and natural phenomena usually leads to partial differential equations (PDEs). PDEs play an important role in applied as well as pure mathematics and they are ubiquitous in describing diverse physical events such as advection, convection, diffusion, heat transfer, conservation laws, acoustics, electromagnetic, etc. Among others, convection-diffusion (CD) equations have been appeared in modelling of several complex events such as smoke plume in atmosphere, migration of contaminants in a stream, tracer dispersion in a porous medium, dispersion of chemicals in reactors, etc [30]. For the most applications of these kinds of model problems, one cannot usually obtain an analytical solution. Thus, it is important to develop numerical algorithms to deal with PDEs models involving CD equations effectively.

*Corresponding author, ORCID: 0000-0002-9277-8092
E-mail: harimsri@math.uvic.ca
DOI: 10.22103/jmmrc.2022.19497.1264

How to cite: H.M. Srivastava, M. Izadi, *The Rothe-Newton approach to simulate the variable coefficient convection-diffusion equations*, J. Mahani Math. Res. Cent. 2022; 11(2): 141-158.

The main goal of this manuscript is to solve a class of CD equations with variable coefficients given by [30]

$$\frac{\partial \mu}{\partial \tau}(x,\tau) + \alpha(x)\,\frac{\partial \mu}{\partial x}(x,\tau) = \beta(x)\,\frac{\partial^2 \mu}{\partial x^2}(x,\tau) + s(x,\tau),\ x \in [0,L], \tau \in [0,T]. \tag{1}$$

The accompanied initial condition is

$$\mu(x,0) = g(x), \quad x \in [0,L], \tag{2}$$

and subject to the boundary conditions

$$\mu(0,\tau) = \mu_0(\tau), \quad \mu(L,\tau) = \mu_L(\tau), \quad \tau \in [0,T]. \tag{3}$$

The coefficient functions $\alpha(x)$ and $\beta(x) \neq 0$ are both continuous in (1), and $s(x,\tau)$ is a given source function. Also, three functions $g(x)$, $\mu_0(\tau)$, and $\mu_1(\tau)$ are known.

Various types of CD have been extensively considered in the literature from both the theoretical and numerical point of view. However, we found that only an operational matrix method based on the second kind Chebyshev wavelets technique [30] proposed for the model (1), to best in our knowledge. Different compuatational algorithms have been develeoped to treat different CD and related equations numerically. Let us review some of them such as the classical finite difference schemes [3, 7–9, 11, 19], the numerical inverse Laplace transform [6], the sinc method [5], the meshless algorithms [17,24], the multiscale-like multigrid technique [20], the spline and B-spline collocation methods [4, 22, 23], the finite element based approximations [1, 2, 4, 8, 18], the upwind finite volume scheme [27], and the Bessel and Chebyshev collocation procedures [25, 28, 29], to name a few.

This article aims to develope a hybrid computational approach to treat the linear IBVP (1)-(3) numerically in an accurate and reliable manner. The proposed combined algorthim is relied on a horizontal line method attributed to Rothe [21] together with new employed Newton polynomials. This implies that we first apply the Rothe method to the IBVP (1)-(3) to get a sequence of time discretized equations, which are continuous with respect to the spatial variable. Hence, the spectral collocation strategy relied on the Newton basis functions is applied to acquire an approximate solutions of the time discretized equations at each time step. Similar approaches using the Taylor series expansion in time and utilizing various (orthogonal) bases inside the spectral collocation technique have been successfully employed to many important and applied PDEs in litearure [10, 12, 13, 15, 16].

The remainder of this research paper has the following organization. We review the Newton functions in Section 2 and then the convergence analysis of them is discussed in a weighted L_2 norm. An illustration of the Rothe temporal time discretization technique is given in Section 3. Section 4 is devoted to the combined Rothe-Newton collocation technique applied to the CD model (1). By solving three numerical test cases, we show the accuracy of the hybrid

method in Section 5. Scope of future works and concluding summary are given in Section 6.

2. Newton basis functions

To proceed, we fix a set of points $X := \{x_0, x_1, \ldots, x_K\}$ on the interval $[0, L]$ in an non-decreasing order. The monic Newton basis functions are defined by

$$N_0(x) \equiv 1, \quad N_k(x) := \prod_{j=0}^{k-1}(x - x_j), \text{ for } k = 1, 2, \ldots, K. \tag{4}$$

Note that the points $x_0, x_1, \ldots, x_K$ are not necessarily distinct. If we have $x_0 = x_1 = \cdots = x_K$, the Newton bases reduces to the well-known Taylor basis at $x = x_0$. Clearly, each basis function $N_k(x)$ is exactly of degree k and therefore the set of Newton basis functions $\{N_k(x)\}_{k=0}^{K}$ forms a basis for the space of polynomials of degree less or equal to K.

2.1. **A convergence result.** We continue by defining $\Omega = [0, L]$. Associating Ω with the weight function $w(x) = 1/L$, we further consider the weighted space $L^2_w(\Omega)$ is defined by [13]

$$L^2_w(\Omega) = \{q : \Omega \to \mathbb{R} \ : \ q \text{ is mesurable and } \|q\|_w < \infty\},$$

where

$$\|q\|^2_w = \int_\Omega |q(x)|^2 \, w(x)dx,$$

is the norm induced from the following inner product of the space $L^2_w(\Omega)$ as

$$\langle q(x), p(x)\rangle_w = \int_\Omega q(x)\, p(x) w(x)dx.$$

Next, let us consider a subspace of $L^2_w(\Omega)$ of finite-dimensional defined by

$$\mathbb{V}_K = \text{span}\langle N_0(x), N_1(x), \ldots, N_K(x)\rangle.$$

Obviously, we have $\dim(\mathbb{V}_K) = K + 1$. One can show that $\mathbb{V}_K$ is a closed subspace of $L^2_w(\Omega)$. Therefore, we see that $\mathbb{V}_K$ is a complete subspace of $L^2_w(\Omega)$. Every function $v \in L^2_w(\Omega)$ has a unique best approximation $v_* \in \mathbb{V}_K$ in the sense that

$$\|v(x) - v_*(x)\|_w \leqslant \|v(x) - u(x)\|_w, \quad \forall u \in \mathbb{V}_K. \tag{5}$$

From the approximation theory, we borrow the following result [26] as follows:

Theorem 2.1. *Let assume that $v \in C^K(\Omega)$ and $P_K(x)$ denotes the corresponding interpolating function at K Chebyshev nodes in the interval Ω. The following upper bound is valid*

$$|v(x) - P_K(x)| \leqslant \frac{L^K \|v\|_\infty}{K!\, 2^{2K-1}}, \quad \forall x \in \Omega,$$

where $\|v\|_\infty := \max_{x\in\Omega} |v^{(K)}(x)|$.

Any given function $v \in L^2_w(\Omega)$ can be written in terms of Newton basis functions. In particular, by restricting ourselves to the finite subspace $\mathbb{V}_K$ of $L^2_w(\Omega)$ we are able to express $v(x)$ in terms of $(K+1)$ Newton bases as

$$v(x) \approx v_K(x) = \sum_{k=0}^{K} c_k \, N_k(x).$$

By defining the error function $e_K(x) = v(x) - v_K(x)$ and using the last Theorem 2.1, we have

Theorem 2.2. *Suppose $v \in L^2_w(\Omega) \cap C^{(K)}(\Omega)$ and let $v_K(x)$ is the best approximation to $v(x)$ out of the space $\mathbb{V}_K$ in the sense of* (5)*. Then, we get*

$$\lim_{K \to \infty} \|e_K(x)\|_w = 0.$$

Proof: According to the fact $v_K(x)$ is the best approximation out of $\mathbb{V}_K$, we get

$$\|e_K(x)\|^2_w = \|v(x) - v_K(x)\|^2_w \leqslant \|v(x) - u(x)\|^2_w, \quad \forall u \in \mathbb{V}_K.$$

Especially, by choosing $u(x) = P_K(x) \in \mathbb{V}_K$, one gets

$$\|e_K(x)\|^2_w \leqslant \|v(x) - P_K(x)\|^2_w = \int_\Omega |v(x) - P_K(x)|^2 \, w(x) dx.$$

In view of Theorem 2.1 with K Chebyshev nodes, we further obtain

$$\|e_K(x)\|^2_w \leqslant \int_\Omega \left| \frac{\|v\|_\infty \, L^K}{K! \, 2^{2K-1}} \right|^2 w(x) dx \leqslant \left[\frac{\|v\|_\infty \, L^K}{K! \, 2^{2K-1}} \right]^2.$$

The proof in completed by approaching K to infinity. ■

3. The Rothe procedure

Firstly, we discretize the CD equation (1) in time. This can be accomplished by employing the idea of Rothe method [21]. Let divide the time domain $[0, T]$ into M subintervals $I_1, I_2, \ldots, I_M$, where $I_m = [\tau_{m-1}, \tau_m]$ for $m = 1, 2, \ldots, M$. Here, the grid points are given by

$$\tau_m := m \Delta\tau, \quad m = 0, 1, \ldots, M,$$

and $\Delta\tau := \tau_m - \tau_{m-1}$ signifies the (uniform) time step. For every $\tau = \tau_m$ we approximate the unknown solution $\mu(x, \tau_m)$ by a function $u_m(x)$. The time derivative $\frac{\partial \mu}{\partial \tau}$ at time level τ_m is approximated by the difference quotient

$$\frac{\partial \mu}{\partial \tau}(x, \tau_m) \approx \frac{u_m(x) - u_{m-1}(x)}{\Delta\tau}. \tag{6}$$

By using the starting function $u_0(x) = g(x)$, we seek the functions $u_1(x)$, $u_2(x), \ldots, u_M(x)$ as the solutions of the following boundary value problems

(BVPs)

$$\begin{cases} \frac{u_m(x)-u_{m-1}(x)}{\Delta\tau} + \alpha(x)\, u'_m(x) = \beta(x)\, u''_m(x) + s_m(x), \\ u_m(0) = \mu_0(\tau_m) =: \mu_0^m, \\ u_m(L) = \mu_L(\tau_m) =: \mu_L^m, \end{cases} \qquad m = 1, 2, \ldots, M,$$

where $s_m(x) = s(x, \tau_m)$. By rearranging the terms in the former equations, we get a sequence of BVPs in the form

$$(7) \quad \begin{cases} -\Delta\tau\, \beta(x)\, u''_m(x) + \Delta\tau\, \alpha(x)\, u'_m(x) + u_m(x) = \Delta\tau\, s_m(x) + u_{m-1}(x), \\ u_m(0) = \mu_0^m, \\ u_m(L) = \mu_L^m, \end{cases}$$

for $m = 1, 2, \ldots, M$.

By solving the foregoing equations (7) subsequently, we get the functions $u_1(x)$, $u_2(x), \ldots, u_M(x)$. Thus, we can construct the so-called *Rothe functions* $\mu_1(x, \tau)$ in the whole domain $(0, L) \times [0, T]$ as

$$(8) \qquad \mu_1(x, \tau) = u_{m-1}(x) + \frac{u_m(x) - u_{m-1}(x)}{\Delta\tau}\, (\tau - \tau_{m-1}),$$

on I_m, $m = 1, 2, \ldots, M$. Obviously, the obtained $\mu_1(x, \tau)$ is a piecewise function with respect to τ for every fixed x. By repeating the above mentioned procedure with time steps $\Delta\tau/2, \Delta\tau/4, \Delta\tau/8, \ldots$, we get a sequence of related Rothe functions $\{\mu_n(x, \tau)\}_{n=1}^{\infty}$ and expect to be convergent toward the true solution μ of the original equation (1).

4. **Rothe-Newton approach**

The time-advancement procedure is already accomplished for the equation (1) and is expressed in terms of BVPs (7), which is continuous with respect to x. The next aim is to solve (7) computationally through using the spectral collocation approach. Thus, we need a set of collocation points, let say C_x. In case of distinct x_k, this collocation set C_x can be taken as X, which are actually the roots of Newton bases. Otherwise, we may use the equidistant points in Ω given by

$$(9) \qquad C_x := \left\{ x_j = \frac{j}{L} \mid j = 0, 1, \ldots, K \right\}.$$

Give the starting function $u_0(x) = g(x)$, suppose that the solution $u_m(x)$ of the discretized equation (8) at time level τ_m can be written as a summation of basis functions which are chosen to be the Newton functions. Therefore, for $m = 1, 2, \ldots, M$ we take

$$(10) \qquad \mathcal{U}_{m,K}(x) = \sum_{k=0}^{K} c_k^m\, N_k(x), \quad x \in \Omega.$$

So, our task is to find the unknowns coefficients c_k^m, for $k = 0, 1, \ldots, K$ at time levels $m \geqslant 1$. By letting

$$\boldsymbol{N}_K(x) = \left[N_0(x) \quad N_1(x) \quad \ldots \quad N_K(x)\right],$$

and

$$\boldsymbol{C}_K^m = \left[c_0^m \quad c_1^m \quad \ldots \quad c_K^m\right]^T,$$

we are able to rewrite (10) in a compact representation form as

$$\mathcal{U}_{m,K}(x) = \boldsymbol{N}_K(x)\,\boldsymbol{C}_K^m. \tag{11}$$

The monic vector $\boldsymbol{N}_K(x)$ of Newton bases is further decomposed as

$$\boldsymbol{N}_K(x) = \boldsymbol{Y}_K(x)\,\boldsymbol{V}_K. \tag{12}$$

Here, we have

$$\boldsymbol{Y}_K(x) = \left[1 \quad x \quad x^2 \quad \ldots \quad x^K\right],$$

and the $(K+1) \times (K+1)$ matrix $\boldsymbol{V}_K = (v_{r,s})_{r,s=0}^K$ with an upper-triangular structure is given by

$$\boldsymbol{V}_K = \begin{pmatrix} 1 & -x_0 & x_0x_1 & -x_0x_1x_2 & \ldots & (-1)^K \prod_{i=0}^{K-1} x_i \\ 0 & 1 & -(x_0+x_1) & x_0x_1+x_0x_2+x_1x_2 & \ldots & (-1)^{K-1} \sum_{i=0}^{K-1} \prod_{\substack{0\leqslant j\leqslant K-1 \\ j\neq i}} x_j \\ 0 & 0 & 1 & -(x_0+x_1+x_2) & \ldots & \vdots \\ \vdots & \vdots & \vdots & \ddots & \ddots & \vdots \\ 0 & 0 & 0 & \ldots & 1 & -\sum_{i=0}^{K-1} x_i \\ 0 & 0 & 0 & \ldots & 0 & 1 \end{pmatrix}.$$

It should stressed that the determinant of $\boldsymbol{V}_K = 1$ independently of which values of x_k are chosen.

In view of two relations (11) and (12), we may write the approximate solution $\mathcal{U}_{m,K}(x)$ in (10) as

$$\mathcal{U}_{m,K}(x) = \boldsymbol{N}_K(x)\,\boldsymbol{C}_K^m = \boldsymbol{Y}_K(x)\,\boldsymbol{V}_K\,\boldsymbol{C}_K^m. \tag{13}$$

By inserting the points of collocation (9) of C_x into (13) we arrive

$$\boldsymbol{U}_m = \boldsymbol{Y}\,\boldsymbol{V}_K\,\boldsymbol{C}_K^m, \qquad \boldsymbol{U}_m = \begin{pmatrix} \mathcal{U}_{m,K}(x_0) \\ \mathcal{U}_{m,K}(x_1) \\ \vdots \\ \mathcal{U}_{m,K}(x_K) \end{pmatrix}, \quad \boldsymbol{Y} = \begin{pmatrix} \boldsymbol{Y}_K(x_0) \\ \boldsymbol{Y}_K(x_1) \\ \vdots \\ \boldsymbol{Y}_K(x_K) \end{pmatrix}. \tag{14}$$

We next show the matrix forms of the first and the second derivatives at the given collocation points C_x as follows.

Lemma 4.1. *The matrix expressions of* $\frac{d}{dx}\mathcal{U}_{m,K}(x)$ *and* $\frac{d^2}{dx^2}\mathcal{U}_{m,K}(x)$ *at the collocation points* (9) *are given by*

$$\boldsymbol{U}_m^{(1)} = \boldsymbol{Y}\,\boldsymbol{G}_K\,\boldsymbol{V}_K\,\boldsymbol{C}_K^m, \qquad \boldsymbol{U}_m^{(1)} = \begin{pmatrix} \mathcal{U}_{m,K}^{(1)}(x_0) \\ \mathcal{U}_{m,K}^{(1)}(x_1) \\ \vdots \\ \mathcal{U}_{m,K}^{(1)}(x_K) \end{pmatrix}, \tag{15}$$

$$\boldsymbol{U}_m^{(2)} = \boldsymbol{Y}\,\boldsymbol{G}_K^2\,\boldsymbol{V}_K\,\boldsymbol{C}_K^m, \qquad \boldsymbol{U}_m^{(2)} = \begin{pmatrix} \mathcal{U}_{m,K}^{(2)}(x_0) \\ \mathcal{U}_{m,K}^{(2)}(x_1) \\ \vdots \\ \mathcal{U}_{m,K}^{(2)}(x_K) \end{pmatrix}, \tag{16}$$

where the matrix $\boldsymbol{G}_K$ *is defined in* (17).

Proof: Firstly, we establish a connection between the vector $\boldsymbol{Y}_K(x)$ and its first and second derivatives. A straightforward multiplication indicates that the derivatives of $\boldsymbol{Y}_K(x)$ can be written in terms of differentiation matrix $\boldsymbol{G}_K$ defined via

$$\frac{d}{dx}\boldsymbol{Y}_K(x) = \boldsymbol{Y}_K(x)\,\boldsymbol{G}_K, \quad \boldsymbol{G}_K = \begin{pmatrix} 0 & 1 & 0 & \dots & 0 \\ 0 & 0 & 2 & \dots & 0 \\ \vdots & \vdots & \ddots & \vdots & \vdots \\ 0 & 0 & 0 & \ddots & K \\ 0 & 0 & 0 & \dots & 0 \end{pmatrix}_{(K+1)\times(K+1)}. \tag{17}$$

In a recursive manner, we get the following relation for the second derivative

$$\frac{d^2}{dx^2}\boldsymbol{Y}_K(x) = \frac{d}{dx}\boldsymbol{Y}_K(x)\,\boldsymbol{G}_K = \boldsymbol{Y}_K(x)\,\boldsymbol{G}_K^2.$$

We now differentiate on both sides of relation (13) twice. By exploiting the foregoing matrix relations we get

$$u'_m(x) \approx \mathcal{U}_{m,K}^{(1)}(x) = \boldsymbol{Y}_K(x)\,\boldsymbol{G}_K\,\boldsymbol{V}_K\,\boldsymbol{C}_K^m, \tag{18}$$

$$u''_m(x) \approx \mathcal{U}_{m,K}^{(2)}(x) = \boldsymbol{Y}_K(x)\,\boldsymbol{G}_K^2\,\boldsymbol{V}_K\,\boldsymbol{C}_K^m. \tag{19}$$

The desired results are gained by substituting the points of collocations (9) into the former relations (18) and (19). ■

For convenience and for $m = 1, 2, \ldots, M$, we define the following coefficients for relation (7) as

$$\begin{aligned} \phi_{2,m}(x) &:= -\Delta\tau\, \beta(x), \\ \phi_{1,m} &:= \Delta\tau\, \alpha(x), \\ h_m(x) &:= s_m(x) + u_{m-1}(x). \end{aligned}$$

Therefore, we can represent the model problem (7) in a compact form as

$$\phi_{2,m}(x)\, u''_m(x) + \phi_{1,m}(x)\, u_m(x) + u_m(x) = h_m(x), \quad x \in \Omega. \tag{20}$$

We next place the approximate solutions $\mathcal{U}_{m,K}(x)$, $\mathcal{U}^{(1)}_{m,K}(x)$, and $\mathcal{U}^{(2)}_{m,K}(x)$ into (20). Thus, we get the following equation for $m = 1, 2, \ldots, M$ as

$$\phi_{2,m}(x)\, \mathcal{U}^{(2)}_{m,K}(x) + \phi_{1,m}(x)\, \mathcal{U}_{m,K}(x) + \mathcal{U}_{m,K}(x) = h_m(x), \quad x \in \Omega. \tag{21}$$

We ultimately get a fundamental matrix equation to find the approximate solutions of discretized model (8) at each time level τ_m as:

Lemma 4.2. *Let for $m = 1, 2, \ldots, m$, the numerical solutions of* (8) *are represented in terms of expansion series* (10)*. Then, we have*

$$\boldsymbol{A}_m\, \boldsymbol{C}^m_K = \boldsymbol{H}_m \qquad or \qquad [\boldsymbol{A}_m; \boldsymbol{H}_m] \tag{22}$$

where

$$\boldsymbol{A}_m := \left\{ \boldsymbol{\Psi}_{2,m}\, \boldsymbol{Y}\, \boldsymbol{G}^2_K + \boldsymbol{\Psi}_{1,m}\, \boldsymbol{Y}\, \boldsymbol{G}_K + \boldsymbol{Y} \right\} \boldsymbol{V}_K,$$

for the unknown coefficients $\boldsymbol{C}^m_K$. Here, the right-hand side vector $\boldsymbol{H}_m$ and the matrices $\boldsymbol{\Psi}_{\ell,m}$, $\ell = 1, 2$ are defined as

$$\boldsymbol{\Psi}_{\ell,m} = \begin{pmatrix} \phi_{\ell,m}(x_0) & 0 & \ldots & 0 \\ 0 & \phi_{\ell,m}(x_1) & \ldots & 0 \\ \vdots & \vdots & \ddots & \vdots \\ 0 & 0 & \ldots & \phi_{\ell,m}(x_K) \end{pmatrix}, \quad \boldsymbol{H}_m = \begin{pmatrix} h_m(x_0) \\ h_m(x_1) \\ \vdots \\ h_m(x_K) \end{pmatrix}.$$

Proof: Using the points of C_x, i.e., (9) as the collocation points inserted in the equation (21) followed by expressing all terms in a matrix representation give us

$$\boldsymbol{\Psi}_{2,m}\, \boldsymbol{U}^{(2)}_m + \boldsymbol{\Psi}_{1,m}\, \boldsymbol{U}^{(1)}_m + \boldsymbol{U}_m = \boldsymbol{H}_m, \quad m = 1, 2, \ldots, M. \tag{23}$$

Here, the coefficient matrices of size $(K+1) \times (K+1)$, and the vector $\boldsymbol{H}_m$ of size $(K+1) \times 1$ are defined as above. We then substitute the matrix expression forms for $\boldsymbol{U}_m$, $\boldsymbol{U}^{(1)}_m$, and $\boldsymbol{U}^{(2)}_m$ as given in relations (14), (15) and (16). Hence, the fundamental matrix equation is obtained as desired. ■

4.1. **Treatments of boundary conditions.** The implementations of the boundary conditions (3) or (7) have not been carried out in the matrix forms. After doing these tasks, two rows of the linear systems (22) will be substituted by two new rows given via the corresponding boundary conditions. Let us first consider the left boundary condition $u_m(0) = \mu_0^m$. In this case, we approach $x \to 0$ in relation (13) yields

$$\widehat{\boldsymbol{A}}_0^m := \boldsymbol{Y}_K(0)\,\boldsymbol{V}_K\,\boldsymbol{C}_K^m = \mu_0^m, \qquad \text{or} \qquad [\widehat{\boldsymbol{A}}_0^m;\ \mu_0^m].$$

Analogously, the right boundary condition $u_m(L) = \mu_L^m$ is converted to the matrix form by approaching $x \to L$ in (13). This gives us

$$\widehat{\boldsymbol{A}}_L^m := \boldsymbol{Y}_K(L)\,\boldsymbol{V}_L\,\boldsymbol{C}_K^m = \mu_L^m, \qquad \text{or} \qquad [\widehat{\boldsymbol{A}}_L^m;\ \mu_L^m].$$

Now, two rows $[\widehat{\boldsymbol{A}}_0^m;\ \mu_0^m]$ and $[\widehat{\boldsymbol{A}}_L^m;\ \mu_L^m]$ will be entered into the linear fundamental matrix equation (22). This task can be accomplished for instance by replacing the first and last rows of $[\boldsymbol{A}_m; \boldsymbol{H}_m]$. Therefore, the following linear algebraic system of equations is obtained

$$\widehat{\boldsymbol{A}}_m\,\boldsymbol{C}_K^m = \widehat{\boldsymbol{H}}_m, \quad \text{or} \quad [\widehat{\boldsymbol{A}}_m,\ \widehat{\boldsymbol{H}}_m]. \tag{24}$$

This implies that through a combined technique, the CD model problem (1) is transformed to a system of linear equations to be solved for the unknowns Newton coefficients c_k^m for $k = 0, 1, \ldots, K$. To this end, at each time level τ_m, a linear-type solver can be used to solve the matrix equation (24) consists of $(K + 1)$ linear equations and $(K + 1)$ unknowns.

5. Numerical examples and experiments

In this section, all calculations are performed using Matlab version R2021a on a digital computer. Three numerical examples are given to testify the obtained theoretical results and the computational effectiveness of the hybrid Rothe-Newton technique applied to the CD equation with variable coefficients. For validation of results a comparison will be drawn between our numerical models and between analytical and numerical outcomes of an existing method.

Numerical errors are measured through defining the absolute errors at time step $\tau = \tau_m$ by

$$E_{m,K}(x) := |\mu(x, \tau_m) - \mathcal{U}_{m,K}(x)|, \quad x \in \Omega,\ m = 1, \ldots, M.$$

The L_∞ and L_2 error norms at the final time $\tau = T$ are also computed via

$$\mathcal{E}_\infty := \max_{0 \leqslant x \leqslant L} E_{M,K}(x), \quad \mathcal{E}_2 := \sqrt{\frac{1}{K+1}\int_0^L [\mu(x,T) - \mathcal{U}_{M,K}(x)]^2 dx}\ .$$

We further compute the numerical rate of convergences (ROC) corresponds to $\mathcal{E}_2$ and $\mathcal{E}_\infty$ as the number of Newton basis functions K and the grid size $\Delta\tau$

are halved successively. By letting $\mathcal{E}_\ell \equiv \mathcal{E}_\ell(M,K)$ for $\ell = 2, \infty$, the ROC with regard to variables τ and x are given by

$$\mathrm{ROC}\tau_\ell := \log_2 \frac{\mathcal{E}_\ell(M,K)}{\mathcal{E}_\ell(2M,K)}, \quad \mathrm{ROC}x_\ell := \log_2 \frac{\mathcal{E}_\ell(M,2K)}{\mathcal{E}_\ell(M,K)}, \quad \ell = 2, \infty.$$

Example 5.1. *Let us consider the CD equations with the following coefficients given by [30]*

$$\alpha(x) = -0.1, \quad \beta(x) = 0.01, \quad s(x,\tau) = 0, \quad x \in [0, L = 1].$$

The initial and boundary conditions on $[0,1]$ *are*

$$g(x) = e^{-x}, \quad \mu_0(\tau) = exp(-0.09\tau), \quad \mu_1(\tau) = exp(-1 - 0.09\tau), \quad \tau \in [0,T].$$

An easy calculation shows that the related analytical solution is $\mu(x,\tau) = exp(-x - 0.09\tau)$.

To begin, we set $K = 5$, and $T = 1$. In this case, we select the collocation points as $C_x = \{0, 0.2, 0.4, 0.6, 0.8, 1\}$. Utilizing a relatively large time step $\Delta\tau = 0.1$ in the hybrid Rothe-Newton collocation algorithm, the following approximate solutions at the first time step $\tau = \Delta\tau$ and the last time step $\tau = T$ are obtained respectively

$$\mathcal{U}_{1,5}(x) = -0.00436079\,x^5 + 0.0355682\,x^4 - 0.160494\,x^3 + 0.49344\,x^2 - 0.99061\,x + 0.99104,$$

and

$$\mathcal{U}_{10,5}(x) = 0.00318853\,x^5 + 0.010729\,x^4 - 0.122898\,x^3 + 0.441696\,x^2 - 0.910429\,x + 0.913931.$$

Graphical representation of the approximate solution in 3D shown in Fig. 1. In addition, the related plot of absolute error is shown in Fig. 1, right panel. We also compute the numerical rate of convergence of the proposed hybrid approach applied to Example 5.1. To confirm the theoretical order of convergences with regard to both time and space variables, we first fix $K = 5$ and use various $\Delta\tau = 1/2^i$ for $i = 1, 2, 3, 4$. Hence, we fix $\Delta\tau = 0.001$ and vary $K = 1, 2, 4, 8$. The achieved $\mathcal{E}_2/\mathcal{E}_\infty$ error norms are reported in Table 1. It can be seen that the order of convergence $\mathcal{O}(\Delta\tau)$ in time and the exponential convergence with respect to the spatial variable are obtained. These results obviously confirm the theoretical order of convergence of the hybrid approach.

To show the capability of the proposed hybrid technique, a comparison is made between the obtained results and the outcomes of the second kind Chebyshev wavelets method (SKCWM) reported in [30] with parameters $k = 2, M = 3$. In Table 2, we tabulate the numerical solutions obtained using $K = 5$, $\Delta\tau = 0.00625$ and evaluated at $t = T = 0.3$. Clearly, a slightly better results are obtained via our straightforward approach rather than SKCWM, which is more complicated in implementation. On the hand, by increasing K or/and decreasing $\Delta\tau$ one obtains more accuracy.

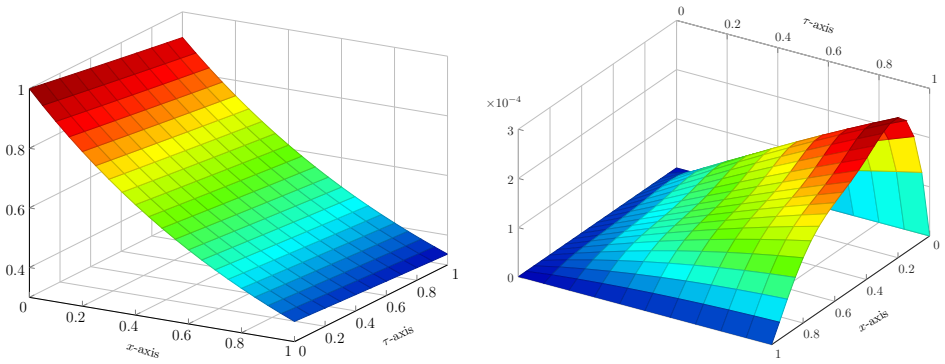

FIGURE 1. The profile of approximate solution (left) and the achieved absolute errors (right) in Example 5.1 for $K = 5, \Delta\tau = 0.1$ on $[0,1] \times [0,1]$.

TABLE 1. The results of $\mathcal{E}_2/\mathcal{E}_\infty$ error norms and the related ROC in Example 5.1 with a fixed $K = 5, \Delta\tau = 0.001$, $T = 1$, and diverse $\Delta\tau, K$ for $x \in [0,1]$.

	$K = 5$					$\Delta\tau = 0.001$			
$\Delta\tau$	$\mathcal{E}_2$	ROCτ_2	$\mathcal{E}_\infty$	ROCτ_∞	K	$\mathcal{E}_2$	ROCx$_2$	$\mathcal{E}_\infty$	ROCx$_\infty$
$\frac{1}{2}$	3.9626_{-4}	–	1.3846_{-3}	–	1	3.6713_{-2}	–	7.1211_{-2}	–
$\frac{1}{4}$	2.0329_{-4}	0.963	7.0628_{-4}	0.971	2	2.0589_{-3}	4.1563	5.7985_{-3}	3.6184
$\frac{1}{8}$	1.0302_{-4}	0.981	3.5673_{-4}	0.985	4	6.8712_{-6}	8.2271	3.5525_{-5}	7.3507
$\frac{1}{16}$	5.1907_{-5}	0.989	1.7929_{-4}	0.993	8	7.1029_{-7}	3.2741	2.9636_{-6}	3.5834

Example 5.2. *The second test case is devoted to the CD equations with variable coefficients as [30]*

$$\alpha(x) = -x/6, \quad \beta(x) = x^2/12, \quad s(x,\tau) = 0, \quad x \in [0, L = 1].$$

The initial and boundary conditions on $[0,1]$ *are*

$$g(x) = x^3, \quad \mu_0(\tau) = 0, \quad \mu_1(\tau) = exp(\tau), \quad \tau \in [0,T].$$

The exact solution is given by $\mu(x,\tau) = exp(\tau)x^3$.

In the second case, we consider again $K = 5$, $T = 1$, but $\Delta\tau = 0.01$. The approximate solutions at three different time steps $\tau = \Delta\tau, T/2, T$ are obtained

TABLE 2. Comparison of numerical/exact solutions in Example 5.1 for $\Delta\tau = 0.00625$, $K = 5$, $T = 0.3$, and diverse $x \in [0, 1]$.

x	$\mathcal{U}_{48,5}(x)$	Exact	$E_{48,5}(x)$	SKCWM [30]
0.1	0.880739097871781	0.880733672597157	5.4252746_{-6}	3.6214847509708_{-6}
0.2	0.796926748644148	0.796920782290140	5.9663540_{-6}	4.5180604012485_{-6}
0.3	0.721089207305733	0.721083743026607	5.4642791_{-6}	4.3421411977107_{-6}
0.4	0.652468534270911	0.652463552227900	4.9820430_{-6}	2.1868871755704_{-6}
0.5	0.590377954206663	0.590373435960464	4.5182462_{-6}	2.5234925130846_{-5}
0.6	0.534195973335112	0.534191975471484	3.9978636_{-6}	1.7603814034262_{-6}
0.7	0.483360496736049	0.483356887821146	3.6089149_{-6}	4.5073975851184_{-6}
0.8	0.437362945649467	0.437359398365983	3.5472835_{-6}	3.0698324923750_{-6}
0.9	0.395742374778093	0.395739148771237	3.2260069_{-6}	8.3723127229374_{-6}

as follows

$$\mathcal{U}_{1,5}(x) = -0.00123167\,x^5 + 0.00244246\,x^4 + 1.0084\,x^3 + 0.000482765\,x^2 - 0.0000461907\,x,$$

$$\mathcal{U}_{50,5}(x) = -0.00935663\,x^5 + 0.00405933\,x^4 + 1.65533\,x^3 - 0.00149678\,x^2 + 0.000182636\,x,$$

and

$$\mathcal{U}_{100,5}(x) = 0.0153816\,x^5 - 0.0626772\,x^4 + 2.77616\,x^3 - 0.0116192\,x^2 + 0.00103341\,x.$$

The profile of approximate solution is visualized in 3D in Fig. 2. Also, the space-time visualization of achieved absolute errors is plotted in Fig. 2, left picture. The computations of ROC related to the second example are also reported in Table 3. Obviously, the numerical order of convergence in time is of first-order while an exponential behaviour is seen with regard to the spatial variable x. The graphs of achieved $\mathcal{E}_2$ and $\mathcal{E}_\infty$ error norms versus K using $\Delta\tau = 0.001$ are shown in Fig. 3.

Example 5.3. *We consider the non-homogenous CD equations having the following coefficients [30]*

$$\alpha(x) = 2, \quad \beta(x) = 1, \quad s(x,\tau) = -2exp(\tau - x), \quad x \in [0, L = 1].$$

The accompanied initial and boundary conditions on $[0, L]$ *are given as*

$$g(x) = exp(-x), \quad \mu_0(\tau) = exp(\tau), \quad \mu_1(\tau) = exp(\tau - 1), \quad \tau \in [0, T].$$

The true exact solution is given by $\mu(x,\tau) = exp(\tau - x)$.

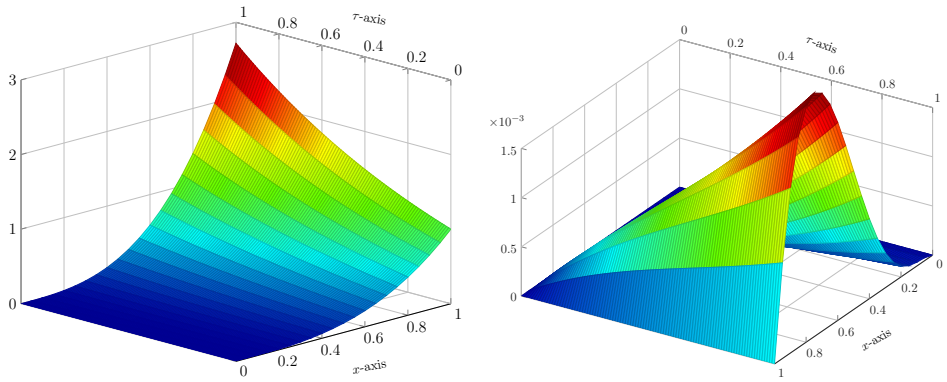

FIGURE 2. The profile of approximate solution (left) and the achieved absolute errors (right) in Example 5.2 for $K = 5, \Delta\tau = 0.01$ on $[0,1] \times [0,1]$.

TABLE 3. The results of $\mathcal{E}_2/\mathcal{E}_\infty$ error norms and the related ROC in Example 5.2 with a fixed $K = 5, \Delta\tau = 0.001$, $T = 1$, and diverse $\Delta\tau, K$ for $x \in [0,1]$.

	$K = 5$					$\Delta\tau = 0.001$			
$\Delta\tau$	$\mathcal{E}_2$	ROCτ_2	$\mathcal{E}_\infty$	ROCτ_∞	K	$\mathcal{E}_2$	ROCx$_2$	$\mathcal{E}_\infty$	ROCx$_\infty$
$\frac{1}{2}$	2.8037_{-2}	–	1.1316_{-1}	–	1	5.3055_{-1}	–	1.0462_{-0}	–
$\frac{1}{4}$	1.4420_{-2}	0.959	5.9024_{-2}	0.939	2	5.5966_{-2}	3.2449	1.5374_{-1}	2.7666
$\frac{1}{8}$	7.3230_{-3}	0.978	3.0232_{-2}	0.969	4	6.5608_{-5}	9.7365	2.4906_{-4}	9.2698

Let us take $K = 5, T = 1$, and $\Delta\tau = 0.01$ in the last test example. We get the approximate solutions at the first, middle, and last time steps $\tau = \Delta\tau, T/2, T$ respectively as follows

$$\mathcal{U}_{1,5}(x) = -0.00489628\,x^5 + 0.0375366\,x^4 - 0.164889\,x^3 + 0.503449\,x^2 - 1.00967\,x + 1.01005,$$

$$\mathcal{U}_{50,5}(x) = -0.00857934\,x^5 + 0.0627902\,x^4 - 0.27132\,x^3 + 0.821444\,x^2 - 1.64653\,x + 1.64872,$$

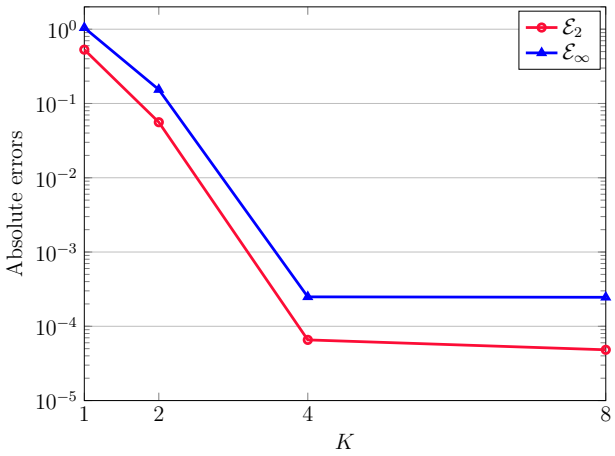

FIGURE 3. Graphs of $\mathcal{E}_2$ and $\mathcal{E}_\infty$ versus K using $\Delta\tau = 0.001$ and $T = 1$.

and

$$\mathcal{U}_{100,5}(x) = -0.0141343\,x^5 + 0.103503\,x^4 - 0.447333\,x^3 + 1.35434\,x^2 - 2.71465\,x + 2.71828.$$

The diagram of approximate solution along the difference between the obtained approximation and the exact solution are presented in Fig. 4. The parameters used as the same as above. Analogously, an investigation of ROC with respect both L_2 and L_∞ is performed in Table 4. Here, we employed $K = 5$ and $\Delta\tau = 1/4, 1/8, 1/16$ for the time variable. Also, we fixed $\Delta\tau = 0.001$ and varied $K = 1, 2, 4$ to prove the exponential convergence of the proposed technique for the spacial variable. Utilizing a large $L = 2$ and $T = 3$, the graphical representation of approximate solution with $K = 5$ and $\Delta\tau = 0.0125$ is depicted in Fig. 5.

6. Conclusions and future works

A novel hybrid technique based on two existing approximation algorithms is proposed to solve a class of variable coefficients convection-diffusion equations arising in diverse disciplines of physical and applied engineering. For time-marching procedure, the idea of Rothe horizontal line method is employed whereas a matrix collocation approach based on well-known Newton basis functions is applied for the spatial variable. We proved that the convergence rate of the Newton spectral method has an exponential bahaviour while the Rothe method is a first-order accurate in time. Three numerical examples are solved to show the utility and applicability of the presented hybrid technique. Generalizing the presented approach to similar model problems, systems of PDEs

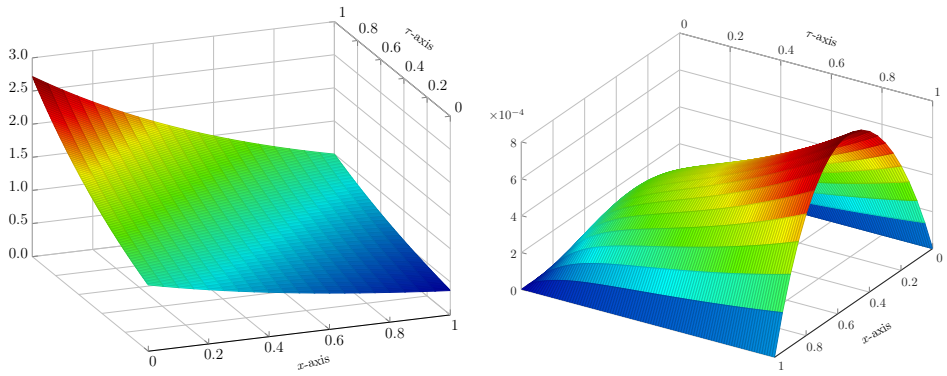

FIGURE 4. The profile of approximate solution (left) and the achieved absolute errors (right) in Example 5.3 for $K = 5, \Delta\tau = 0.01$ on $[0,1] \times [0,1]$.

TABLE 4. The results of $\mathcal{E}_2/\mathcal{E}_\infty$ error norms and the related ROC in Example 5.3 with a fixed $K = 5, \Delta\tau = 0.001$, $T = 1$, and diverse $\Delta\tau, K$ for $x \in [0,1]$.

	$K = 5$					$\Delta\tau = 0.001$			
$\Delta\tau$	$\mathcal{E}_2$	ROCτ_2	$\mathcal{E}_\infty$	ROCτ_∞	K	$\mathcal{E}_2$	ROCx$_2$	$\mathcal{E}_\infty$	ROCx$_\infty$
$\frac{1}{4}$	6.4721_{-3}	–	2.1544_{-2}	–	1	1.0919_{-1}	–	2.1180_{-1}	–
$\frac{1}{6}$	3.3600_{-3}	0.946	1.1182_{-2}	0.946	2	1.0114_{-2}	3.4324	2.8682_{-2}	2.8845
$\frac{1}{16}$	1.7124_{-3}	0.972	5.6976_{-3}	0.973	4	6.5829_{-5}	7.2635	2.0664_{-4}	7.1169

and higher-order PDEs is straightforward. These are worthy of investigations for conducting future works.

References

[1] M. Ahmadinia, Z. Safari, S. Fouladi, Analysis of local discontinuous Galerkin method for time-space fractional convection-diffusion equations, BIT Numer. Math. Vol. 58, no. 3, (2018) 533–554

[2] M. Ahmadinia, Z. Safari, Convergence analysis of a LDG method for tempered fractional convection-diffusion equations, ESAIM: Math. Model. Numer. Anal. Vol. 54, no. 1, (2020) 59-78.

[3] C. Clavero, J.C. Jorge, F. Lisbona, A uniformly convergent scheme on a nonuniform mesh for convection-diffusion parabolic problems, J. Comput. Appl. Math. Vol. 154, (2003) 415–429.

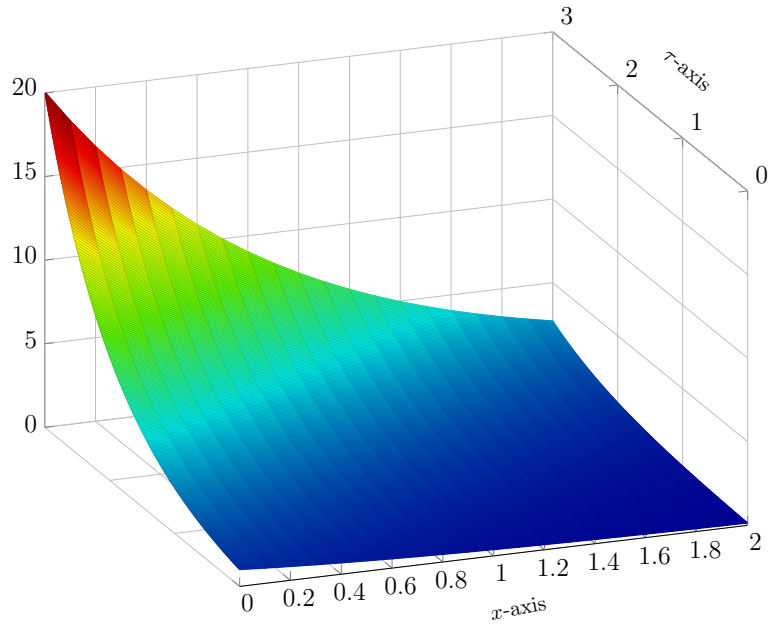

FIGURE 5. The profile of approximate solution in Example 5.3 for $K = 5, \Delta\tau = 0.0125$ for $(x, \tau) \in [0, 2] \times [0, 3]$

[4] S. Dhawan, S. Kapoor, S. Kumar, Numerical method for advection diffusion equation using FEM and B-splines, J. Comput. Sci. Vol. 3, (2012) 429–437.
[5] A. Fahim, M. A. Fariborzi Araghi, Numerical solution of convection-diffusion equations with memory term based on sinc method, Comput. Methods Differ. Equ. Vol. 6, no. 3, (2018) 380–395.
[6] N. Guglielmi, M. López-Fernández, G. Nino, Numerical inverse Laplace transform for convection-diffusion equations, Math. Comp. Vol. 89, (2020) 1161–1191.
[7] M. Izadi, Split-step finite difference schemes for solving the nonlinear Fisher equation, J. Mahani Math. Res. Cent. Vol. 7, no. 1-2, (2018) 37–55.
[8] M. Izadi, Application of the Newton-Raphson method in a SDFEM for inviscid Burgers equation, Comput. Methods Differ. Equ. Vol. 8, no. 4, (2020) 708–732.
[9] M. Izadi, A second-order accurate finite-difference scheme for the classical Fisher-Kolmogorov-Petrovsky-Piscounov equation, J. Infor. Optim. Sci. Vol. 42, no. 2, (2021) 431–448.
[10] M. Izadi, A combined approximation method for nonlinear foam drainage equation, Sci. Iran. Vol. 29, no. 1, (2022) 70–78.
[11] M. Izadi, Two-stages explicit schemes based numerical approximations of convection-diffusion equations, Int. J. Comput. Sci. Math. (2022) in press.
[12] M. Izadi, P. Roul, Spectral semi-discretization algorithm for a class of nonlinear parabolic PDEs with applications, Appl. Math. Comput. Vol. 429, (2022) Article ID 127226.
[13] M. Izadi, M.E. Samei, Time accurate solution to Benjamin-Bona-Mahony Burgers equation via Taylor-Boubaker series scheme, Bound. Value Probl. Vol. 2022, (2022) Article ID 17.

[14] M. Izadi, H.M. Srivastava, An optimized second order numerical scheme applied to the non-linear Fisher's reaction-diffusion equation, J. Interdiscip. Math. Vol. 25, no. 2, (2022) 471–492.
[15] M. Izadi, Ş. Yüzbaşı, A hybrid approximation scheme for 1-D singularly perturbed parabolic convection-diffusion problems, Math. Commun. Vol. 27, no. 1, (2022) 47–63.
[16] M. Izadi, Ş. Yüzbaşı, D. Baleanu, A Taylor-Chebyshev approximation technique to solve the 1D and 2D nonlinear Burgers equations, Math. Sci. (2021), https://doi.org/10.1007/s40096-021-00433-1,
[17] C.Y. Ku, J.E. Xiao, C.Y. Liu, Space-time radial basis function-based meshless approach for solving convection-diffusion equations, Mathematics, Vol. 8 no. 10, (2020) Article ID 1735.
[18] N. Okhovati, M. Izadi, Numerical coupling of two scalar conservation laws by a RKDG method, J. Korean Soc. Ind. Appl. Math. Vol. 23, no. 3, (2019) 211–236.
[19] N. Okhovati, M. Izadi, A predictor-corrector scheme for conservation equations with discontinuous coefficients, J. Math. Fund. Sci. Vol. 52, no. 3, (2020) 322-338.
[20] M. Li, Z. Zheng, An efficient multiscale-like multigrid computation for 2D convection-diffusion equations on nonuniform grids, Math. Methods Appl. Sci. Vol. 44, no. 4, (2021) 3214–3224.
[21] E. Rothe, Zweidimensionale parabolische randwertaufgaben als grenzfall eindimensionaler randwertaufgaben, Math. Ann. Vol. 102, no. 1, (1930) 650–670.
[22] H.S. Shekarabi, J. Rashidinia, Three level implicit tension spline scheme for solution of Convection-Reaction-Diffusion equation, Ain Shams Eng. J. Vol. 9, (2018) 1601–1610.
[23] H. S. Shukla, M. Tamsir, An exponential cubic B-spline algorithm for multi-dimensional convection-diffusion equations, Alexandria Eng. J. Vol. 57, no. 3, (2018) 1999–2006.
[24] H. M. Srivastava, H. Ahmad, I. Ahmad, P. Thounthong, M. N. Khan, Numerical simulation of 3-D fractional-order convection-diffusion PDE by a local meshless method, Thermal Sci. Vol. 25 no. (1A), (2021) 347–358.
[25] H. M. Srivastava, H. I. Abdel-Gawad, K. M. Saad, Oscillatory states and patterns formation in a two-cell cubic autocatalytic reaction-diffusion model subjected to the Dirichlet conditions, Discrete Contin. Dyn. Syst. S Vol. 14 (2021), 3785–3801.
[26] G.W. Stewart, Afternotes on Numerical Analysis, SIAM, Vol. 49, 1996.
[27] J. Tan, An upwind finite volume method for convection-diffusion equations on rectangular mesh, Chaos Solit. Fract. Vol. 118, (2019) 159–165.
[28] V. M. Tripathi, H. M. Srivastava, H. Singh, C. Swarup, S. Aggarwal, Mathematical analysis of non-isothermal reaction-diffusion models arising in spherical catalyst and spherical biocatalyst, Appl. Sci. Vol. 11 (2021), Article ID 10423.
[29] Ş. Yüzbaşı, N. Sahin, Numerical solutions of singularly perturbed one-dimensional parabolic convection-diffusion problems by the Bessel collocation method, Appl. Math. Comput. Vol. 220, (2013) 305–315.
[30] F. Zhou, X. Xu. *Numerical solution of the convection diffusion equations by the second kind Chebyshev wavelets*, Appl. Math. Comput. Vol. 247, (2014) 353–367.

Hari Mohan Srivastava
Orcid number: 0000-0002-9277-8092
[1]Department of Mathematics and Statistics, University of Victoria,
Victoria, British Columbia V8W 3R4, Canada
[2]Department of Medical Research, China Medical University Hospital,
China Medical University, Taichung 40402, Taiwan, Republic of China
[3]Department of Mathematics and Informatics, Azerbaijan University,
71 Jeyhun Hajibeyli Street, AZ1007 Baku, Azerbaijan
[4]Section of Mathematics, International Telematic University Uninettuno,
I-00186 Rome, Italy
Email address: harimsri@math.uvic.ca

Mohammad Izadi
Orcid number: 0000-0002-6116-4928
[5]Department of Applied Mathematics
Faculty of Mathematics and Computer
Shahid Bahonar University of Kerman
Kerman, Iran
Email address: izadi@uk.ac.ir